Mössbauer spectra of CoZn-substituted *Z*-type barium ferrite $Ba_3Co_{2-x}Zn_xFe_{24}O_{41}$

Z. W. Li* and Lin Guoqing
Temasek Laboratories, National University of Singapore, 10 Kent Ridge Crescent, Singapore, 119260

Nai-Li Di and Zhao-Hua Cheng
State Key Laboratory of Magnetism, Institute of Physics, Chinese Academy of Sciences, Beijing 100080, People's Republic of China

C. K. Ong
Center for Superconducting and Magnetic Materials and Department of Physics, National University of Singapore, 10 Kent Ridge Crescent, Singapore, 119260

(Received 24 January 2005; revised manuscript received 4 April 2005; published 9 September 2005)

Mössbauer spectra of powder and aligned $Ba_3Co_{2-x}Zn_xFe_{24}O_{41}$ samples with $x=0-2.0$ have been obtained and analyzed at room temperature and at $T=7$ K with applied magnetic fields of 0 and 60 kOe. The relationship between Mössbauer parameters and magnetic properties has been studied. The magnetocrystalline anisotropy of $Ba_3Co_{2-x}Zn_xFe_{24}O_{41}$ is modified from the *c* plane to the *c* axis at Zn concentration $x=1.2-1.6$, based on the dependence of the quadrupole splitting and hyperfine field on Zn substitution for powder samples, and the values of the angle factor *b* for aligned samples. Zn ions occupy only sites with down spin, while Co ions prefer sites with up spin. As the Zn substitution increases, the increase in saturation magnetization is attributed to the occupation of Zn ions at sites with down spin, which decreases the negative magnetization, thus increasing the net magnetization.

DOI: 10.1103/PhysRevB.72.104420 PACS number(s): 76.80.+y, 75.50.Gg, 75.30.−m

I. INTRODUCTION

In the hexagonal ferrite family, *M*-type barium ferrites have been extensively used as permanent magnets for low cost and perpendicular recording materials. Other interesting hexagonal ferrites, *W*-type, *Y*-type, and *Z*-type barium ferrites, are used in microwave devices or electromagnetic attenuation materials at high frequency. These barium ferrites have more complicated crystal structure and magnetic properties than the *M*-type ferrite, and were originally investigated by Jonker *et al.*[1] Co_2Z barium ferrite, $Ba_3Co_2Fe_{24}O_{41}$, is one of the more important barium ferrites. Co_2Z has complex spin re-orientation. As the temperature decreases from the Curie temperature to 490 K, it is modified from uniaxial to planar anisotropy, and is changed to a cone anisotropy for $T<230$ K.[2] At room temperature, Co_2Z has a *c*-plane anisotropy with a large out-of-plane anisotropy field of 12 000 Oe and a small in-plane anisotropy field of about 120 Oe.[3,4] Therefore Co_2Z is a good soft magnetic material with large permeability and high resonance frequency (1.5 GHz),[5,6] thus can be considered for use as electromagnetic (EM) materials with low reflectivity and broad bandwidth at microwave frequency.

However, the saturation magnetization M_s of Co_2Z is slightly low, only 51 emu/g at room temperature. With Zn substitution for Co, M_s increases smoothly but significantly to 59 emu/g for Zn_2Z ferrite, $Ba_3Zn_2Fe_{24}O_{41}$.[7] The increase of 15% in M_s is significantly superior to that of *M*- and *W*-type barium ferrites. For *M*-type ferrites, Zn substitution can lead to a slight increase (below 2%) in M_s.[8,9] For CoZn substituted *W*-type ferrites, M_s first increases to a smooth maximum at Zn concentration of 0.6, and then decreases with further Zn substitutions.[10] The increase in M_s has often been attributed to the occupation of nonmagnetic Zn ions at sites with spin-down for spinel ferrites[11] and *M*-type barium ferrites.[9,11] However, this assumption has been not proven in experiments on *Z*-type ferrites.

The unit cell of the *Z*-type barium ferrite consists of four *S* blocks (spinel block without barium ions), two *R* blocks (hexagonal block comprising barium ions and two oxygen layers), and two *T* blocks (hexagonal block comprising barium ions and four oxygen layers), and can be described as the sequence of $RSTSR^*S^*T^*S^*$, where the asterisk indicates a rotation of 180° around the *c*-axis for the corresponding block. There are ten inequivalent crystallographic sites, $12k_{VI}$, $2d_V$, $4f_{VI}$, $4f_{VI}$, $4e_{VI}$, $4f_{IV}$, $12k^*_{VI}$, $2a_{VI}$, $4e_{VI}$, and $4f^*_{IV}$ sites, based on the standard Wyckoff notations. The crystallographic and magnetic characteristics of the ten sites are listed in Table I.[12]

Magnetic properties, such as Curie temperature, saturation magnetization, and magnetic anisotropy, are found to be strongly influenced by the distribution of metallic ions at the sites for spinel or barium ferrites.[9,13–15] Mössbauer spectroscopy and neutron diffraction are useful experimental techniques to study the magnetic properties at each site and the ion distributions at various sites. Numerous papers have been published on the studies of Mössbauer spectra for *M*- and *W*-type barium ferrites. However, only few considered the Mössbauer spectra of *Z*-type barium ferrites.[2] In this work, a comprehensive study on the Mössbauer spectra for CoZn substitution *Z*-type barium ferrites, $Ba_3Co_{2-x}Zn_xFe_{24}O_{41}$ with $x=0-2$, is performed. An increase in the saturation magnetization with Zn substitutions is observed. Based on the metallic ion distributions at the various sites, the origin for the increase in magnetization is investigated.

TABLE I. Coordination, block location, the number of ions per formula unit, and spin direction in *Z*-type barium ferrite (Ref. 2).

Site	Coordination	Block	Number of ions	Spin	Component
$12k_{VI}$	octahedral	*R-S*	6	up	
$2d_V$	fivefold	*R*	1	up	I
$4f_{VI}$	octahedral	*R*	2	down	
$4e_{VI}$	octahedral	*T*	2	down	
$4e_{IV}$	tetrahedral	*S*	2	down	II+IV
$4f_{IV}$	tetrahedral	*S*	2	down	
$4f^*_{IV}$	tetrahedral	*T*	2	down	
$4f^*_{VI}$	octahedral	*S*	2	up	
$12k^*_{VI}$	octahedral	*T-S*	6	up	III
$2a_{VI}$	octahedral	*T*	1	up	

II. EXPERIMENT

Samples of $Ba_3Co_{2-x}Zn_xFe_{24}O_{41}$ with $x=0$, 0.4, 0.8, 1.2, 1.6, and 2.0 were synthesized using the conventional ceramic technique. A mixture of $BaCO_3$, Fe_2O_3, Co_3O_4, and ZnO in the appropriate ratio required for *Z*-type barium ferrite was calcined at 1300 °C for 3 h. The calcined samples were then crushed and ball-milled. Finally, the powders were shaped and sintered at 1300 °C for 6 h.

X-ray diffraction has shown that all $Ba_3Co_{2-x}Zn_xFe_{24}O_{41}$ samples, with $x=0-2.0$, are single phase with *Z*-type hexagonal structure. The structural parameters and magnetic properties are shown in Table II.

Two types of samples were prepared for Mössbauer spectra measurements. The powder samples were prepared by embedding the powders of $Ba_3Co_{2-x}Zn_xFe_{24}O_{41}$ in epoxy resin. All samples contained about 4–5 mg/cm^2 of natural iron. The aligned samples were prepared by mixing fine powders of $Ba_3Co_{2-x}Zn_xFe_{24}O_{41}$ with epoxy resin in a cylindrical mold of 20 mm diameter and thickness of about 2 mm, followed by placing the mold in applied fields of 3–6 kOe. The volume concentration was below 5%. The powders can rotate freely in the epoxy. Upon curing of the epoxy, the magnetic field was removed and all particles were aligned along a crystallographic direction. The plane of the aligned samples is normal to the alignment direction.

TABLE II. Crystal structural and magnetic parameters of $Ba_3Co_{2-x}Zn_xFe_{24}O_{41}$. *a* and *c* are lattice parameters, *V* is the volume of the unit cell, M_s is the specific saturation magnetization, H_c is the coercivity, and χ_p is the high-field susceptibility.

x	a nm	c nm	c/a	V nm^3	M_s emu/g	H_c Oe	χ_p emu/g/kOe
0.0	0.588	5.257	8.93	1.576	51.9	26	0.029
0.4	0.589	5.264	8.94	1.582	53.5	17	0.028
0.8	0.589	5.273	8.95	1.586	55.2	15	0.029
1.2	0.590	5.277	8.95	1.590	56.1	14	0.031
1.6	0.590	5.281	8.94	1.594	58.8	95	0.030
2.0	0.591	5.282	8.94	1.595	58.8	138	0.035

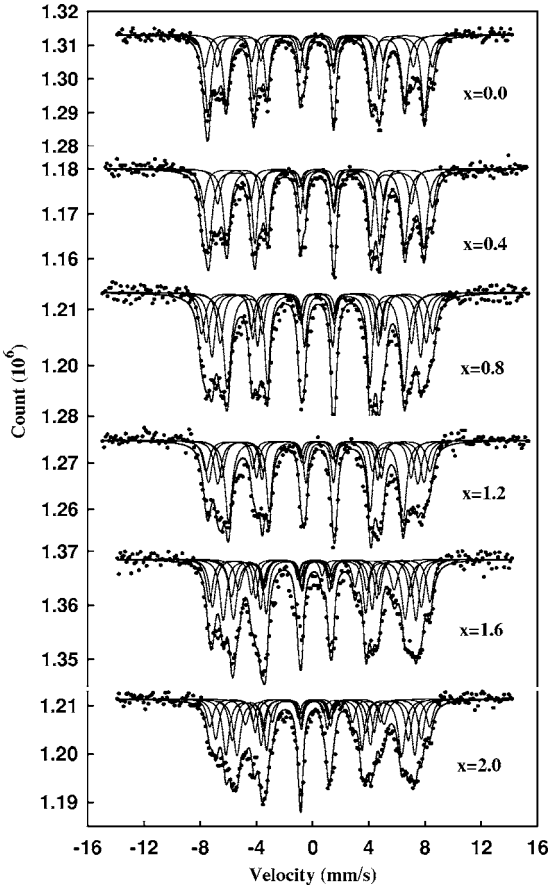

FIG. 1. Mössbauer spectra at room temperature and the curve-fitted results for $Ba_3Co_{2-x}Zn_xFe_{24}O_{41}$.

^{57}Mössbauer spectra were taken at room temperature and at 7 K with a longitudinal magnetic field of 60 kOe using a conventional constant-acceleration spectrometer. The γ-ray source was ^{57}Co in an Rh matrix. Calibration was performed using the α-Fe spectrum.

III. RESULTS

A. Analysis of Mössbauer spectra

Mössbauer spectra at room temperature together with their curve-fitted plots are shown in Fig. 1 for $Ba_3Co_{2-x}Zn_xFe_{24}O_{41}$ with $x=0-2.0$. The points in the figure are the experimental spectra and the solid lines represent the curve-fitted results.

The Mössbauer spectra of $Ba_3Co_{2-x}Zn_xFe_{24}O_{41}$ should be a superposition of at least ten components, corresponding to ten inequivalent crystallography sites. Here, only four distinguishable components, namely I, II, III, and IV, were used to fit the Mössbauer spectrum of $Ba_3Co_{2-x}Zn_xFe_{24}O_{41}$. Further decomposition will lead to a certain extent of indeterminancy. From the analysis of Albanese *et al.*[2] on the Mössbauer of Co_2Z, the ten sites are divided into three groups, as shown in Table I. The octahedral $12k_{VI}$ with up spin and octahedral $4f_{VI}$ with down spin are assigned to component I, the tetragonal $4e_{IV}$, $4f_{IV}$, and $4f^*_{IV}$ sites with down spin are

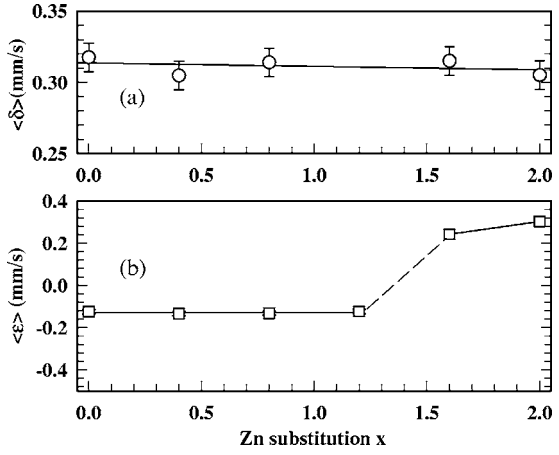

FIG. 2. Mössbauer parameters for $Ba_3Co_{2-x}Zn_xFe_{24}O_{41}$, the averaged (a) isomer shift $\langle\delta\rangle$, and (b) quadrupole splitting $\langle\epsilon\rangle$.

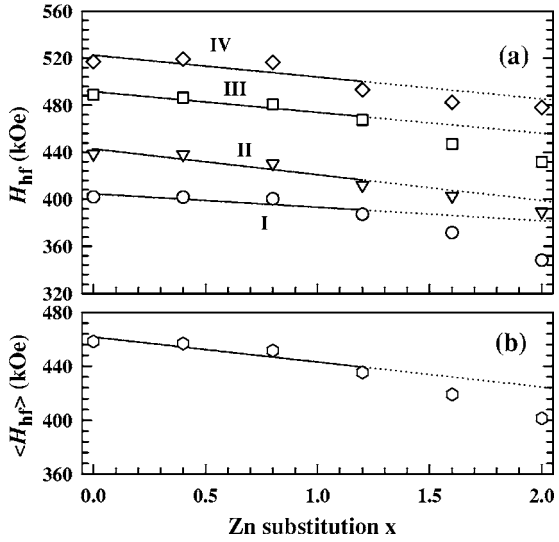

FIG. 3. Hyperfine fields H_{hf} of four components and the averaged field $\langle H_{hf}\rangle$ for $Ba_3Co_{2-x}Zn_xFe_{24}O_{41}$.

assigned to components II and IV, and the octahedral $4f_{VI}^*$, $12k_{VI}^*$, and $2a_{VI}$ with up spin to component III. The validity of these assignments has been proven by the Mössbauer spectra with an applied magnetic field.[2] Based on the area of Mössbauer subspectra, the $2d_V$ with up spin is assigned to component I, and $4e_{VI}$ with down spin is assigned to components II and IV. For higher substitution of Zn ions, components I and III may be decomposed into two subcomponents, which involve $12k_2$ and $12k_2^*$ sites, respectively. The subspectrum for the $12k$ sites is known to decompose into two or three subcomponents, corresponding to various ion neighboring configurations at the $12k$ sites in nonmagnetic ion substituted M-type barium ferrites.[16,17]

B. Mössbauer parameters at room temperature

The isomer shifts (δ) and quadrupole splittings (ϵ) averaged over four components are shown in Figs. 2(a) and 2(b), respectively, as a function of CoZn substitutions. Within experimental error, the isomer shifts $\langle\delta\rangle$ is found to be a constant of 0.31 mm/s, which is the typical value of Fe^{3+} with high spin.

The dependence of quadrupole splittings on CoZn substitution provides important information on the change in the type of magnetic anisotropy, namely c-axis and c-plane anisotropy. When x varies from 0 to 1.2, $\langle\epsilon\rangle$ can be considered as linear to a good approximation. However, for samples with $x \geqslant 1.6$, there is sudden jump in magnitude and a change in sign. The values of $\langle\epsilon\rangle$ are -0.12 mm/s at $x=1.2$ and $+2.4$ mm/s at $x=1.6$. It is well known that the quadrupole splitting ϵ is related to the angle θ between the direction of hyperfine fields and the principal axis of the electric-field gradient (EFG) by

$$\epsilon = \frac{1}{4} eqQ(3\cos^2\theta - 1), \tag{1}$$

where Q is the nuclear quadrupole moment and q is the z component of the EFG along the principal axis. When the magnetic moments of Fe ions are either along the c axis or in the c plane, quadrupole splitting will have significantly different sign and magnitude, due to different θ. Therefore the dependence of $\langle\epsilon\rangle$ on Zn substitutions, as shown in Fig. 2(b), indicates that the magnetic anisotropy of $Ba_3Co_{2-x}Zn_xFe_{24}O_{41}$ is modified from the c plane to the c axis at $x=1.2-1.6$.

The dependence of hyperfine fields on CoZn substitutions, as shown in Figs. 3(a) and 3(b), has two main characteristics:

(i) The hyperfine fields H_{hf} of the four components, as well as the hyperfine field $\langle H_{hf}\rangle$ averaged over the four components, decrease with Zn substitutions. As nonmagnetic Zn ions replace Co ions, the Fe moment will be reduced, thus decreasing the Fermi contact field, which is the dominant component of the hyperfine field.

(ii) The hyperfine fields at each site and the averaged hyperfine field are linear to a good approximation, for $x=0-1.2$. However, at $x=1.6$ and 2.0, the hyperfine fields of components deviate from the straight line, especially for components I and III. It is noted that at $x=1.2-1.6$, the anisotropy of $Ba_3Co_{2-x}Zn_xFe_{24}O_{41}$ is modified from the c-plane to the c axis. Therefore it appears that the deviation can be attributed to the change in the anisotropy dipole field.[18] Similar characteristics in the hyperfine field have also been observed in CoZr substituted M-type barium ferrites.[14]

C. Mössbauer spectra at 7 K and in $H=60$ kOe

The Mössbauer spectrum at 7 K without applied magnetic fields can be fitted by a subspectrum, due to the almost similar values of hyperfine fields at all sites for low temperature.[19–21] The hyperfine fields are 531.6 and 505.0 kOe for Co_2Z and Zn_2Z ferrites, respectively. Under applied fields, the Mössbauer spectrum is divided into two components, associated with small and large hyperfine fields, respectively. They correspond to two spin states of Fe ions: up spin and down spin. The Mössbauer spectra and their curve-fitted results under applied magnetic fields of 60 kOe are shown in Fig. 4 for (a) Co_2Z and (b) Zn_2Z barium ferrite,

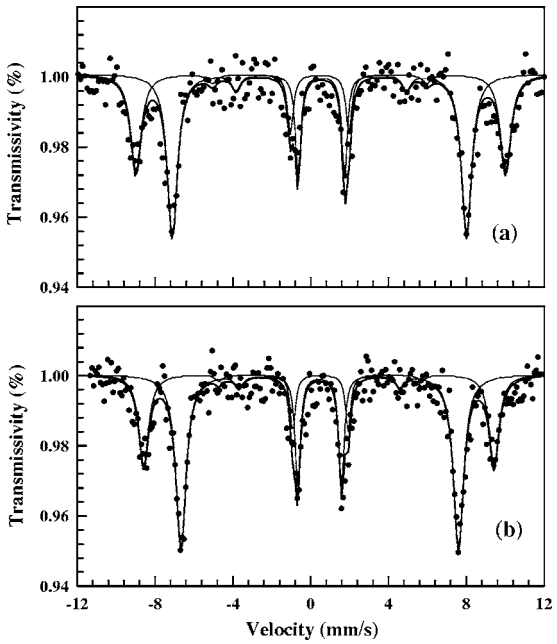

FIG. 4. Mössbauer spectra and the curve-fitted results with an applied field of 60 kOe at $T=7$ K for (a) $Ba_3Co_2Fe_{24}O_{41}$ and (b) $Ba_3Zn_2Fe_{24}O_{41}$, respectively.

respectively. The curve-fitted Mössbauer parameters are listed in Table III.

The occupation numbers of Fe ions with down spin and up spin are given by

$$\begin{cases} N_{\text{down-spin}} = C_{\text{Fe}} S_{\text{down-spin}}/100 \\ N_{\text{up-spin}} = C_{\text{Fe}} S_{\text{up-spin}}/100 \end{cases}, \tag{2}$$

where $C_{\text{Fe}}=24$ is the composition of Fe ions in the chemical formula. Based on Mössbauer spectra and Eq. (2), the occupation numbers of Fe ions with down spin and up spin are calculated to be 8.1 and 15.9, respectively, for Zn_2Z ferrite. For Co_2Z ferrite, these numbers are 9.3 and 14.7, respectively. In addition, as the total occupation numbers of metallic ions are 10 and 16 for down spin and up spin, respectively, as shown in Table I, it is concluded that the 0.7-Co ions occupy sites with down spin and 1.3-Co ions occupy sites with up spin. Zn ions are located only at sites with down spin.

The effective field H_{eff}, the hyperfine field H_{hf}, and the applied field H_0 are related as follows:

$$H_{\text{eff}}^2 = H_{\text{hf}}^2 + H_0^2 + 2H_{\text{hf}}H_0 \cos\beta, \tag{3}$$

where H_{eff} is the effective hyperfine field with applied magnetic field of 60 kOe, H_{hf} is the hyperfine field without applied field, and β is the angle between H_{hf} and H_0. Based on Eq. (3), the calculated values of β, as listed in Table III, are considered to be zero or nearly zero within experimental error.

Also, β can be obtained from the angle factor b by

$$\cos\beta = \sqrt{\frac{4-b}{4+b}}, \tag{4}$$

where b is defined as the ratio of the intensities of the sum of the second and fifth lines to that of the third and fourth lines. The curve-fitted value of b and the calculated β are listed in Table III. Within experimental errors, the value of b is considered to be zero.

Therefore Co_2Z and Zn_2Z ferrites have collinear magnetic structure. This conclusion is also supported by the results of high-field susceptibility χ_p. The low and almost similar values of χ_p for all samples, as listed in Table II, show the collinear magnetic structure.

D. Mössbauer spectra for aligned samples at room temperature

Some typical Mössbauer spectra at room temperature together with curve-fitted results are shown in Fig. 5 for aligned samples with $x=0$, 0.8, and 2.0. In fitting these Mössbauer spectra, all isomer shifts, quadrupole splitting, hyperfine fields, linewidths, and the ratios of the areas of the subspectra were constrained to be the same as those for the corresponding nonaligned samples. However, the ratio of the six absorption lines in each sextet was assumed to be $3:b:1:b:3$, where b is the fitted parameter.

The Mössbauer spectra with $x=0$ and 0.8 are significantly different from the spectrum with $x=2.0$. The intensities of the second and fifth lines are considerably stronger for samples with $x=0$ and 0.8; however, these lines almost disappear for the sample with $x=2.0$. This implies different types of magnetic anisotropy for samples with $x=0$ and 0.8, and sample with $x=2.0$.

TABLE III. Mössbauer parameters for Co_2Z and Zn_2Z barium ferrite. H_{hf} is the hyperfine field, b is the ratio of area for the second and fifth peaks to the third and fourth peaks, S is the subspectral area, and β is the angle between H_{hf} and H_0. Data with superscripts 1 and 2 are obtained from Eqs. (3) and (4), respectively.

			H_{hf} (kOe)	b	S	β^1	β^2
Co_2Z	$H=0$		531.6(16)	2.0	100		
	$H=60$ kOe	down spin	592.5(12)	0.23(56)	38.8(2.4)	11(15)°	19(20)°
		up spin	471.5(10)	0.23(56)	61.2(2.5)	3(10)°	19(20)°
Zn_2Z	$H=0$		505.0(8)	2.0	100		
	$H=60$ kOe	down spin	564.4(10)	0.16(39)	33.7(2.4)	9(11)°	16(20)°
		up spin	444.8(6)	0.16(39)	66.3(2.5)	4(20)°	16(20)°

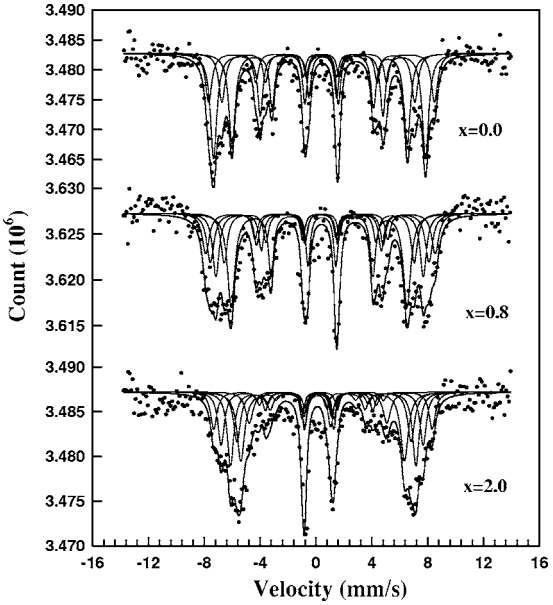

FIG. 5. Mössbauer spectra and the curve-fitted results at room temperature for aligned samples of $Ba_3Co_{2-x}Zn_xFe_{24}O_{41}$ with $x=0$, 1.2, and 2.0.

Reference 14 showed that Mössbauer spectra of aligned samples can be used to distinguish the c-axis and c-plane anisotropies of barium ferrites, based on the angle factor b,

$$b = \frac{4\sigma^2}{2-\sigma^2}, \tag{5}$$

for c-axis anisotropy, and

$$b = \frac{4(1+\sigma^2)}{3-\sigma^2} \tag{6}$$

for c-plane anisotropy. In the above equations, σ^2 is the mean-square deviation of Fe magnetic moment to the alignment direction. For fully aligned samples ($\sigma=0$), based on Eqs. (5) and (6), the angle factor b is 0 and 4/3 for c-axis anisotropy and c-plane anisotropy, respectively. For nonfully aligned samples, the mean deviation σ can be calculated from the two equations.

As shown in Table IV, the curve-fitted values of b are 1.44 and 1.41, which are close to 4/3, for samples with $x=0$ and 1.2, respectively, while $b=0.56$ is almost zero for the sample with $x=2.0$. These values imply that the samples with $x=0$ and 1.2 have c-plane anisotropy and the sample with $x=2.0$ has c-axis anisotropy, consistent with the conclusions

TABLE IV. Mössbauer parameters for the aligned $Ba_3Co_{2-x}Zn_xFe_{24}O_{41}$ with $x=0$, 1.2, and 2.0. b is the angle factor, σ is the mean deviation.

x	b	σ (deg)	Anisotropy
0.0	1.44(10)	14(6)°	c plane
1.2	1.41(10)	12(7)°	c plane
2.0	0.56(22)	28(5)°	c axis

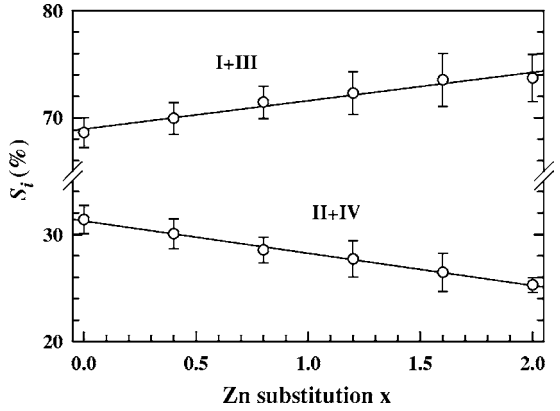

FIG. 6. The areas of Mössbauer subspectra I+III and II+IV for $Ba_3Co_{2-x}Zn_xFe_{24}O_{41}$.

obtained from the dependence of the quadrupole splitting and the hyperfine field on the concentration of Zn. In addition, the mean deviation σ is also obtained from Eqs. (5) and (6), and are listed in Table IV.

IV. DISCUSSIONS AND CONCLUSIONS

The fitted relative areas of the Mössbauer subspectrum are shown in Fig. 6 for components I+III and II+IV. The total occupation numbers of CoZn ions at sites associated with subspectra I+III and II+IV can be calculated from

$$\begin{cases} N_{\text{Co-Zn}}(\text{I}+\text{III}) = 18 - C_{\text{Fe}}(S_{\text{I}}+S_{\text{III}})/100 \\ N_{\text{Co-Zn}}(\text{II}+\text{IV}) = 8 - C_{\text{Fe}}(S_{\text{II}}+S_{\text{IV}})/100 \end{cases}, \tag{7}$$

respectively, where $C_{\text{Fe}}=24$ is the composition of Fe ions in the chemical formula. Among the 26 metallic ions, 18 ions are associated with subspectra I and III, and 8 ions are linked to subspectra II and IV. The calculated results are listed in Table V. Subspectra I and III are related to sites with up spin, except for the $4f_{\text{VI}}$ site, while subspectra II and IV are related to sites with down spin. As the Zn substitution increases, the total number of Co and Zn ions decreases for up spin, and increases for down spin. Therefore Zn ions preferentially occupy sites with down spin, while Co ions prefer sites with up spin.

TABLE V. The occupation numbers of Zn, Co, and Fe ions on the sites with down spin and up spin calculated from the Mössbauer subspectra.

x	0	0.4	0.8	1.2	1.6	2.0
$N_{\text{Co+Zn}}$(I+III)	1.5	1.2	0.9	0.7	0.4	0.1
$N_{\text{Co+Zn}}$(II+IV)	0.5	0.8	1.1	1.3	1.6	1.9
N_{Zn}(up)	0	0	0	0	0	0.1
N_{Zn}(down)	0	0.4	0.8	1.20	1.6	1.9
N_{Co}(up)	1.4	1.1	0.8	0.6	0.3	0
N_{Co}(down)	0.6	0.5	0.4	0.2	0.1	0
N_{Fe}(up)	14.6	14.9	15.2	15.4	15.7	15.9
N_{Fe}(down)	9.4	9.1	8.8	8.6	8.3	8.1

This conclusion is consistent with the experimental results of *M*-type, *W*-type, and *Y*-type barium ferrites. The Mössbauer spectra of $LaZnFe_{11}O_{19}$ showed that 90% of the Zn ions are located on the $4f_{IV}$ sites, which have a tetragonal symmetry and down spin.[22] Li and co-workers[9,14] have shown that Zn ions preferentially occupy the $4f_{VI}$ site with down spin and Co ions prefer the $12k$ site with octahedral structure, based on the Mössbauer of ZnZr and CoZr substituted *M*-type barium ferrites. In $BaZn_2Fe_{16}O_{27}$, Zn ions are located at the $4e$ and $4f_{IV}$ tetrahedral sites of the *S* block, as confirmed by the Mössbauer spectra.[23] Neutron diffraction of $BaFe_{1-2x}Zn_xTi_xO_{19}$ indicated that the ZnTi ions occupy the $4f_{VI}$, $4f_{IV}$, $12k$, and $2b$ sites, but exclude the $2a$ site for low Zn-Ti substitutions.[24]

On the other hand, Co ions showed preference for the octahedral $12k$ site with up spin in *M*- and *W*-type barium ferrites,[14,15,17,25,26] and also occupied the octahedral $4f_{VI}$ site, in spite of the down spin for the site.[17] The neutron-diffraction data obtained from the single crystal indicated that Co ions are mainly located in the octahedral and tetrahedral sites of the *S* block in $BaCo_2Fe_{16}O_{27}$.[27] Albanese *et al.*[28] have shown that Co ions preferred octahedral sites in Co_2Y barium ferrite; 0.9-Co ions occupy the $6c_{VI}$ with down spin and 1.1-Co ions distribute among the $3a_{VI}$, $18h_{VI}$, and $3b_{VI}$ sites with up spin. In Co_2Z barium ferrite, 1.08-Co ions occupy sites with up spin, while the residual 0.92-Co ions distribute over the octahedral $4f_{VI}$ and $4e_{VI}$ sites with down spin.[2] Recent neutron diffraction has shown that Co ions occupy only $12k_{VI}$, $2d_V$, $2a_{VI}$, and $4e_{IV}$ sites out of ten possible sites in $Ba_3Co_{2-x}Fe_{24+x}O_{41}$.[29]

Based on Mössbauer experiments and the above analysis, it is reasonable to make the following conclusions: (i) in $Ba_3Co_{2-x}Zn_xFe_{24}O_{41}$, Zn ions only occupy the $4f_{IV}$, $4f^*_{IV}$, and $4f_{VI}$ tetragonal sites, which are associated with down spin (or subspectrum II and IV); (ii) Co ions preferentially occupy the $12k_{VI}$ of *R*-*S* block with up spin, and can also be located at the octahedral $4f_{VI}$ site of the *R* block or octahedral $4e_{VI}$ site of the *T* block, which have down spin.

The distributions of Zn, Co, and Fe ions over the up-spin and down-spin sites can be calculated as follows: (i) Zn ions are located only at sites with down spin. The number of Zn ions is zero at sites with up spin. (ii) By subtracting the number of Zn ions from the total number of CoZn ions, we can obtain the number of Co ions at sites associated with subspectra I+III and subspectra II+IV, respectively. (iii) since only the $4f_{VI}$ site has down spin among sites associated with subspectra I+III, Co ions of 2/16 are considered to have down spin, and the others to have up spin. (iv) The numbers of Fe ions with down spin and up spin can be calculated from the total number of ions, subtracting the number of Co and Zn ions in the two cases, respectively. The calculated results are listed in Table V, and shown in Fig. 7. For Co_2Z ferrite, Co ions of 1.4 and 0.6 occupy sites with up spin and down spin, respectively. For Zn_2Z ferrite, almost all Zn ions are located at sites with down spin. The results are supported by Mössbauer spectra under an applied field of 60 kOe for Co_2Z and Zn_2Z ferrites (see Sec. III C).

The averaged hyperfine fields with various Zn substitutions are shown in Fig. 3(b). It is known that the moment of the Fe atom (or ion) is approximately proportional to the hyperfine field for many series of magnetic materials. Assuming that the proportionality coefficient is κ, the total moment n_B, in chemical formula, is given by

$$n_B = \kappa H_{hf}(N_{Fe}\uparrow - N_{Fe}\downarrow) + \mu_{Co}(N_{Co}\uparrow - N_{Co}\downarrow). \quad (8)$$

The result of $n_B/(N_{Co}\uparrow - N_{Co}\downarrow)$, as a function of $H_{hf} \times (N_{Fe}\uparrow - N_{Fe}\downarrow)/(N_{Co}\uparrow - N_{Co}\downarrow)$, is shown in Fig. 8(a). A good linear relationship between both is observed. From the

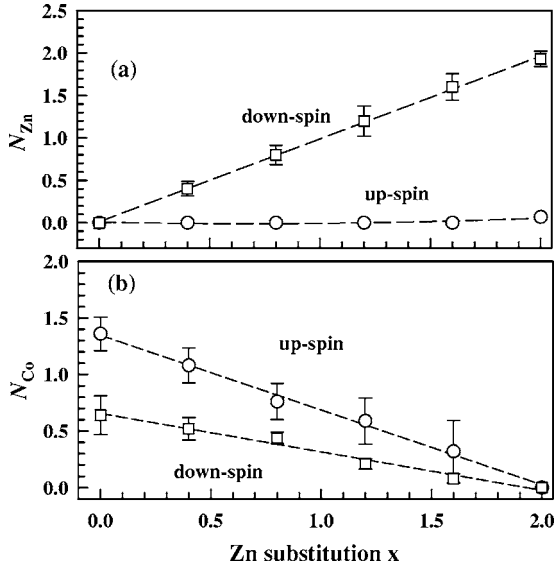

FIG. 7. The occupation numbers of (a) Zn and (b) Co ions at sites with down spin and up spin.

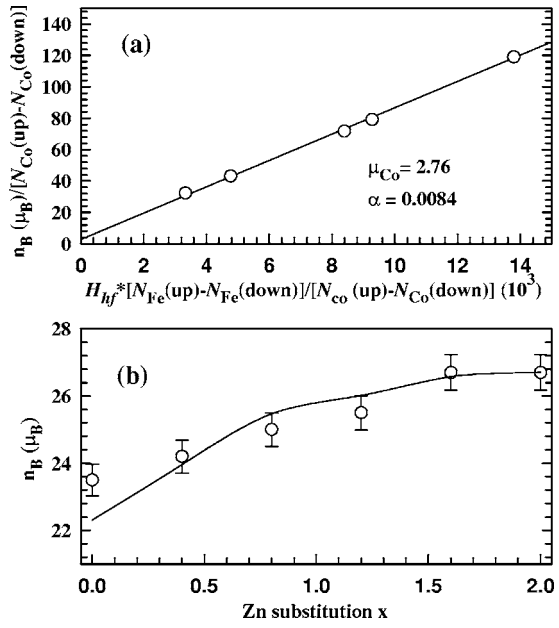

FIG. 8. (a) The relationship between the net magnetic moment per chemical formula, n_B, and the product of hyperfine field and occupation numbers of Fe ions with up spin and down spin, $H_{hf} \times (N_{Fe}\uparrow - N_{Fe}\downarrow)$, in the unit of $(N_{Co}\uparrow - N_{Co}\downarrow)^{-1}$, and (b) calculated (solid line) and experimental (open circles) n_B for $Ba_3Co_{2-x}Zn_xFe_{24}O_{41}$.

slope and intercept of the line, we obtain the averaged moment of Co ions, $\mu_{Co}=2.76\ \mu_B$, and the coefficient, $\kappa=8.40\times10^{-3}\ \mu_B/\text{kOe}$. The calculated coefficient κ is close to $\kappa=9.1\times10^{-3}\mu_B/\text{kOe}$ found at the *B* site for various spinel ferrites.[30] The theoretical value of $\mu_{Co^{2+}}$ is $3\mu_B$ at 0 K, if the orbital moment is quenched. Therefore it is reasonable to have the curve-fitted Co moment of $2.76\mu_B$ at room temperature.

Further, based on Eq. (8) and the distributions of Fe and Co ions over sites with down spin and up spin, the total moment n_B per chemical formula is calculated for $Ba_3Co_{2-x}Zn_xFe_{24}O_{41}$. The calculated results are shown as a solid line in Fig. 8(b), which is consistent with experimental data (open circles).

In conclusion, from the areas of the Mössbauer subspectra, Zn ions only occupy sites with down spin, and Co ions prefer sites with up spin. As the Zn substitution increases, the increase in saturation magnetization can be attributed to the occupation of Zn ions at sites with down spin, which reduces the negative magnetization, thereby increasing the net magnetization. In addition, Mössbauer spectra showed that the magnetocrystalline anisotropy of $Ba_3Co_{2-x}Zn_xFe_{24}O_{41}$ is modified from the *c* plane to the *c* axis for concentration of Zn, $x=1.2-1.6$, based on the dependence of the quadrupole splitting and hyperfine field on the Zn substitution for powder samples, and the angle factor *b* for aligned samples.

ACKNOWLEDGMENT

One of the authors, Dr. Z. H. Cheng, thanks the Alexander von Humboldt Foundation for financial support and generous donation of some Mössbauer equipment.

*Electronic address: tsllizw@nus.edu.sg

[1] G. W. Jonker, H. P. J. Wijn, and P. B. Braun, Philips Tech. Rev. **18**, 145 (1954).
[2] G. Albanese, A. Deriu, and S. Rinaldi, J. Phys. C **9**, 1313 (1976).
[3] J. Verwell, in *Magnetic Properties of Materials*, edited by J. Smit (McGraw-Hill, New York, 1971), p. 64.
[4] C. Jacquiod and D. Autissier, J. Magn. Magn. Mater. **104–107**, 419 (1992).
[5] R. A. Braden, I. Gordon, and R. L. Harvey, IEEE Trans. Magn. **2**, 43 (1966).
[6] T. Nakamura and E. Hankui, J. Magn. Magn. Mater. **257**, 158 (2003).
[7] J. Smit and H. P. J. Wijn, *Ferrites* (Philips Technical Library, Eindhoven, 1959).
[8] C. S. Wang, F. L. Wei, M. Lu, D. H. Han, and Z. Yang, J. Magn. Magn. Mater. **183**, 241 (1998); H. C. Fang, Z. Yang, C. K. Ong, Y. Li, and C. S. Wang, *ibid.* **187**, 129 (1998).
[9] Z. W. Li, C. K. Ong, Z. Yang, F. L. Wei, X. Z. Zhou, J. H. Zhao, and A. H. Morrish, Phys. Rev. B **62**, 6530 (2000).
[10] P. Paoluzi, F. Licci, O. Moze, G. Turilli, A. Deriu, G. Albanese, and E. Calabrese, J. Appl. Phys. **63**, 5074 (1988).
[11] S. Musić, in *Mössbauer Spectroscopy of Sophisticated Oxides*, edited by A. Vértes and Z. Homonnay (Akadémiai Kiadó, Budapest, 1997), p. 88.
[12] M. Sugimoto, in *Ferromagnetic Materials*, edited by E. P. Wohlfarth (North-Holland, Amsterdam, 1982), Vol. 3, p. 393.
[13] A. H. Morrish, Z. W. Li, and X. Z. Zhou, J. Phys. I **7**, C1-513 (1997).
[14] Z. W. Li, L. Chen, X. Rao, and C. K. Ong, Phys. Rev. B **67**, 054409 (2003).
[15] X. Z. Zhou, A. H. Morrish, Z. Yang, and H. X. Zeng, J. Appl. Phys. **75**, 5556 (1994).
[16] G. Albanese, M. Carbuciccho, and G. Asti, J. Appl. Phys. **11**, 81 (1976); G. Albanese, A. Deriu, E. Lucchini, and G. Slokar, Appl. Phys. A: Solids Surf. **26**, 45 (1981).
[17] X. Z. Zhou, A. H. Morrish, Z. W. Li, and Y. K. Hong, IEEE Trans. Magn. **27**, 4654 (1991).
[18] F. van der Would, Phys. Status Solidi **17**, 417 (1966).
[19] J. S. van Wieringen and J. G. Rensen, Z. Angew. Phys. **21**, 69 (1966); J. S. van Wieringen, Philips Tech. Rev. **28**, 33 (1967).
[20] M. Drofenik, D. Hanzel, and A. Moljik, J. Mater. Sci. **8**, 924 (1973).
[21] K. Haneda and A. H. Morrish, IEEE Trans. Magn. **25**, 2597 (1989).
[22] X. Obradors, A. Isalgue, A. Collomb, A. Labarta, M. Pernet, J. A. Pereda, J. Tejada, and J. C. Joubert, J. Phys. C **19**, 6605 (1986).
[23] A. Collomb and M. Vallet-Regi, Mater. Res. Bull. **22**, 753 (1987).
[24] P. Wartewig, M. K. Krause, P. Esquinazi, S. Rösler, and R. Sonntag, J. Magn. Magn. Mater. **192**, 83 (1999).
[25] D. G. Agresti, T. D. Shelfer, Y. K. Hong, and Y. J. Paig, IEEE Trans. Magn. **25**, 4069 (1989).
[26] A. R. Corradi, D. E. Speliotis, A. H. Morrish, Q. A. Pankhurst, X. Z. Zhou, G. Bottoni, D. Candolfo, A. Cecchetti, and F. Masoli, IEEE Trans. Magn. **24**, 2862 (1988).
[27] A. Collomb, B. Lambert-Andron, J. X. Boucherle, and D. Samaras, Phys. Status Solidi A **96**, 385 (1986).
[28] G. Albanese, M. Carbucicchio, and A. Deriu, Appl. Phys. **7**, 227 (1975).
[29] T. Tachibana, T. Nakagawa, Y. Takada, K. Izumi, T. A. Yamamoto, T. Shimada, and S. Kawano, J. Magn. Magn. Mater. **262**, 248 (2003).
[30] F. van der Woude and G. A. Sawatzky, Phys. Rev. B **4**, 3159 (1971).